

A Double Layer Electromagnetic Cloak And GL EM Modeling

Ganquan Xie* and Jianhua Li, Feng Xie, Lee Xie†

GL Geophysical Laboratory, USA

(Dated: October 24, 2018)

In this paper, we propose a novel electromagnetic (EM) cloaking structure that consists of two annular layers between three spherical shells and model its performance numerically and theoretically by using a Global and Local EM field (GL) method. The two annular layers contain distinct cloaking materials: the outer layer provides invisibility; the inner layer is fully absorbing. The cloaking materials are weakly degenerative. The wavefield from an EM source located outside the cloak propagates as in free space outside the outer shell, never be disturbed by the cloak and does not penetrate into the inner absorbing layer and concealment. The field of a source located inside inner layer or the cloaked concealment is completely absorbed by the inner layer and never reaches the outside of the middle shell. Moreover, the EM wavefield excited in concealment is not disrupted by the cloak. There exists no Maxwell EM wavefield can be excited in a single layer cloaked concealment which is filled by normal material. Moreover, we find a negative dielectric and positive susceptibility metamaterial to fill into the concealment, such that the interior EM wave propagates from the concealment to free space through the single layer cloak. Therefore, the double layer cloak is important for complete invisibility. Numerical simulations and theoretical analysis verifying these properties are performed using the GL EM modeling method that we described in this paper.

PACS numbers: 13.40.-f, 41.20.-q, 41.20.jb, 42.25.Bs

I. INTRODUCTION

We propose a novel kind of electromagnetic (EM) double layer cloaking structure (a “Double Layer EM cloak”) that consists of two annular layers between three spherical shells, $R_1 \leq r \leq R_2$ and $R_2 \leq r \leq R_3$. Distinct metamaterials are situated in the two layers: the material in the outer layer has properties that provide invisibility, while material in the inner layer is fully absorbing, which can also be useful for making a complete absorption boundary condition. We analyze the performance of the double layer cloak using a Global and Local EM field modeling “GL method” in time domain that we developed in this paper, its versions in frequency domain have been developed in our other papers [1-3]. Pendry et al. [4] proposed a single layer EM cloak material by using a coordinate transformation and ray tracing in 2006. In their cloak, the ray being bending and re-direction around central sphere object and cannot penetrate into it. The cloak device like the vacuum and does not disturb exterior wave field. Later papers studied 2-D plane wave propagation through a cloaking layer are published in Physical review etc. Journals; Mie scattering analytical method for the sphere cloak is studied in [5]; Numerical methods, including finite-difference time-domain method in [6] and finite-element method in [7] are presented in which many relative research work papers are cited. Most researchers paid attention for exterior EM wave field propagation through the cloak. Two authors

have studied the cloak’s effect on sources located inside concealed region [8] and [9]. The authors of [8] stated that “when these conditions are over-determined, finite energy solutions typically do not exist.” They wrote that the single layer cloak is insufficient and proposed a double coating to solve this problem. However, there also is disputing for this problem. In many numerical simulations using the GL method, we discovered and verified cases where a field satisfying Maxwell’s equations cannot be excited by a local source inside of the single layer cloaked concealment which is filled with normal materials. For the above case of EM field excited inside the concealment, our simulations are either divergent or become chaotic when the field propagates to the inner boundary of the single cloaking layer. These simulations remind us to prove that there exists no Maxwell EM wavefield can be excited by source inside of the single layer cloaked concealment which is filled by normal material. The theoretical proof of the statement is proved in this paper by using the GL method. Moreover, we find a negative dielectric and positive susceptibility metamaterial to fill into the concealment, such that the interior EM wave propagates from the concealment to free space through the single layer cloak. Therefore, the double layer cloak is important for complete invisibility.

The double layer cloak proposed here overcomes these difficulties described above by situating a second, absorbing layer inside the outer cloaking layer. The wavefield excited from an EM source located outside the cloak propagates as in free space outside the outer shell and never be disturbed by the cloak; it propagates around and through the outer layer cloak material and does not penetrate into the inner layer and innermost concealment. The field of a source located inside inner layer or the

*Also at GL Geophysical Laboratory, USA, glhua@glgeo.com

†Electronic address: GLGANQUAN@GLGEO.COM

cloaked concealment is completely absorbed by the inner layer and never reaches the outside of the middle shell. Un Maxwell physical behavior at the inner boundary of single cloaking layer does not appear in our simulations of the double layer cloak. The EM wavefield excited in concealment is not disrupted and has no reflection by the double layer cloak. In which the EM environment in the concealment is kept to be normal and has no be changed. As a result, a double layer EM cloak appears to be more thoroughly concealing and more robust than single layer structures. Moreover, the metamaterials situated in the double layer cloak are weakly degenerative.

The analytical method and numerical method for physical simulation have been developed separately in history. The GL method consistently combines both analytical and numerical approaches. The GL method does not need to solve large matrix equations, it only needs to solve 3×3 and 6×6 matrix equations. Moreover, the GL method does not prescribe any artificial boundary, and does not need a PML absorption condition to truncate the infinite domain. The Finite Element Method (FEM) and Finite Difference Method (FDM) have numerical dispersions which confuse and contaminate the physical dispersion in the dispersive metamaterials. The frequency limitation is also a difficulty of FEM and FDM. The ray tracing is used for wave direction only that is not suitable to study full wave field propagation.

The GL method is a significant scattering process which reduces the numerical dispersion and is suitable to simulate physical wavefield scattering in the materials, in particular, for dispersive materials. Born approximation is a conventional method in the quantum mechanics and solid state physics. However, it only has one iteration in the whole domain which may not be accurate in the high frequency and high contrast materials. The GL method divides the domain as a set of sub-domains or sub-lattices which are as small as accurate requirement. The Global field is updated by the local field from the interaction between the global field and local sub-domain materials successively. Once all sub-domain materials are scattered, the GL field solution obtained turn out to be more accurate than the Born approximation. Moreover, the GL method can be mesh-less, including arbitrary geometry sub-domains, such as rectangle, cylindrical and spherical coordinate mixed coupled together. It is full parallel algorithm. The GL method advantages help overcome many historical obstacles described in detail in [1]. The theoretical foundation of the GL method is described in the paper [2]. In particular, for the radial dependent cloak materials, the GL method can be reduced to the system of the one dimensional GL processes in radial interval $[R_1, R_3]$ by using spherical harmonics expansion. We have used the GL modeling [1-2] and inversion technique in [3] to simulate many radial cloak metamaterials, nanometer materials, periodic photonic crystals etc. These simulations show that the GL method is fast and accurate.

The introduction is described in Section 1. The rest

of this paper is organized as follows: Section 2 describes the geometry and material properties of the proposed double layer cloak. Section 3 contains a brief description of the EM integral equations and their solution by the GL method. These equations are used in Section 4 to prove certain theorems about double layer and single layer cloaks. Section 5 shows numerical simulations of the double layer cloak described in Section 2. The advantages of The GL cloak and GL modeling are presented in Section 6. Section 7 presents our conclusions.

II. DOUBLE LAYER ELECTROMAGNETIC CLOAK

In this section, by simulations using GL EM modeling and inversion in time domain which is presented in next section, we propose a novel electromagnetic (EM) cloaking structure that consists of two annular layers between three spherical shells. An inner layer EM anisotropic cloak metamaterial is situated in the inner annular layer; Outer layer EM cloak material is situated in outer layer.

A. Inner Layer EM Anisotropic Cloak Material

On the inner sphere annular layer domain, $\Omega_I = \{r : R_1 \leq r \leq R_2\}$, we propose an anisotropic material as follows,

$$\begin{aligned} [D]_I &= \text{diag} [\bar{\epsilon}_i, \bar{\mu}_i], \\ \bar{\epsilon}_i &= \text{diag} [\epsilon_{r,i}, \epsilon_{\theta,i}, \epsilon_{\phi,i}] \epsilon_0, \\ \bar{\mu}_i &= \text{diag} [\mu_{r,i}, \mu_{\theta,i}, \mu_{\phi,i}] \mu_0, \\ \epsilon_{r,i} &= \mu_{r,i} = \frac{(R_2-r)}{r^2} \left(R_1 + \log \frac{R_2-R_1}{R_2-r} \right)^2 \\ \epsilon_{\theta,i} &= \epsilon_{\phi,i} = \mu_{\theta,i} = \mu_{\phi,i} = \frac{1}{R_2-r}, \end{aligned} \quad (1)$$

The Ω_I is called as the inner layer cloak, the material, $[D]_I = \text{diag} [\bar{\epsilon}_i, \bar{\mu}_i]$ in (1), is the anisotropic inner layer cloak metamaterial. The field of a source located inside inner layer or the cloaked concealment is completely absorbed by the inner layer and never reaches the outside of the middle shell, also, the EM wavefield excited in concealment is not disrupted by the cloak. The inner layer metamaterial, in equation (1), cloaks outer space from the local field excited in the inner layer and concealment, which can also be useful for making a complete absorption boundary condition to truncate infinite domain in numerical simulation.

B. Outer Layer Anisotropic Cloak Material

Let the outer sphere annular domain $\Omega_O = \{r : R_2 \leq r \leq R_3\}$ be the outer layer cloak with the fol-

lowing anisotropic outer layer cloak material,

$$\begin{aligned}
[D]_O &= \text{diag} [\bar{\varepsilon}_o, \bar{\mu}_o], \\
\bar{\varepsilon}_o &= \text{diag} [\varepsilon_{r,o}, \varepsilon_{\theta,o}, \varepsilon_{\phi,o}] \varepsilon_0, \\
\bar{\mu}_o &= \text{diag} [\mu_{r,o}, \mu_{\theta,o}, \mu_{\phi,o}] \mu_0, \\
\varepsilon_{r,o} &= \mu_{r,o} = \frac{R_3}{r} \frac{r^2 - R_2^2}{r^2} \frac{\sqrt{r^2 - R_2^2}}{\sqrt{R_3^2 - R_2^2}}, \\
\varepsilon_{\theta,o} &= \mu_{\theta,o} = \varepsilon_{\phi,o} = \mu_{\phi,o} \\
&= \frac{R_3}{\sqrt{R_3^2 - R_2^2}} \frac{r}{\sqrt{r^2 - R_2^2}}.
\end{aligned} \tag{2}$$

Outer layer cloak provides invisibility, does not disturb exterior EM wave field, and cloaks the concealment from the exterior EM wavefield.

C. GL Double Layer Cloak

The inner cloak Ω_I domain and outer cloak Ω_O domain are bordering on the sphere annular surface $r = R_2$. We assemble the Ω_I as the inner sphere annular domain and Ω_O as the outer sphere annular domain and make them coupling on their interface boundary annular surface $r = R_2$ as follows,

$$\begin{aligned}
\Omega_{GL} &= \Omega_I \cup \Omega_O \\
&= \{r : R_1 \leq r \leq R_2\} \cup \{r : R_2 \leq r \leq R_3\} \\
&= \{r : R_1 \leq r \leq R_3\},
\end{aligned} \tag{3}$$

and situate the Double Layer anisotropic dielectric and susceptibility tensors $[D]_{GL}$ on the Ω_{GL} as follows,

$$[D]_{GL} = \begin{cases} [D]_I, r \in \Omega_I \\ [D]_O, r \in \Omega_O. \end{cases} \tag{4}$$

The double layer EM cloak materials $[D]_I = \text{diag} [\bar{\varepsilon}_i, \bar{\mu}_i]$ in (1) on the Ω_I and outer layer cloak material $[D]_O = \text{diag} [\bar{\varepsilon}_o, \bar{\mu}_o]$ in (2) on Ω_O are assembled into the doubled layer cloak material $[D]_{GL}$ on the domain Ω_{GL} . The domain Ω_{GL} with the metamaterial $[D]_{GL}$ in (4) is called as the double layer cloak which is named GL cloak (GLC). GL cloak means that the outer layer has invisibility, never disturb exterior wavefield and cloaks the Local concealment from the exterior Global field, while the inner layer cloaks outer Global space from interior wavefield excited in the Local concealment. The properties of the double layer material are studied by GL method simulations and analysis in next sections.

D. GLPS Double Layer Cloak

To compare the properties between the GLO cloak and PS cloak, we use the GLI cloak, in equation (1), as inner layer and the PS cloak in [4] with the following anisotropic dielectric and susceptibility,

$$\begin{aligned}
[D]_{PS} &= \text{diag} [\bar{\varepsilon}_{ps}, \bar{\mu}_{ps}], \\
\bar{\varepsilon}_{ps} &= \text{diag} [\varepsilon_{r,p}, \varepsilon_{\theta,p}, \varepsilon_{\phi,p}] \varepsilon_0, \\
\bar{\mu}_{ps} &= \text{diag} [\mu_{r,p}, \mu_{\theta,p}, \mu_{\phi,p}] \mu_0, \\
\varepsilon_{r,p} &= \mu_{r,p} = \frac{R_3}{R_3 - R_2} \frac{(r - R_2)^2}{r^2}, \\
\varepsilon_{\theta,p} &= \varepsilon_{\phi,p} = \varepsilon_{\phi,p} = \mu_{\phi,p} = \frac{R_3}{R_3 - R_2},
\end{aligned} \tag{5}$$

as the outer layer in (4) to construct a GLPS double layer cloak.

E. A Single Negative Refraction Metamaterial

For studying the EM wavefield excited by source inside a concealment which is cloaked by a single layer cloak, we propose and situate a following negative dielectric and positive susceptibility metamaterial,

$$\begin{aligned}
[D]_{GN} &= \text{diag} [\bar{\varepsilon}_{gn}, \bar{\mu}_{gn}], \\
\bar{\varepsilon}_{gn} &= \text{diag} [\varepsilon_r, \varepsilon_{\theta}, \varepsilon_{\phi}] \varepsilon_0, \\
\bar{\mu}_{gn} &= \text{diag} [\mu_r, \mu_{\theta}, \mu_{\phi}] \mu_0, \\
\varepsilon_r &= - \left(\frac{\sqrt{R_1^2 - r^2}}{r} \right)^3, \\
\varepsilon_{\theta} &= \varepsilon_{\phi} = - \frac{r}{\sqrt{R_1^2 - r^2}}, \\
\mu_r &= \left(\frac{\sqrt{R_1^2 - r^2}}{r} \right)^3, \\
\mu_{\theta} &= \mu_{\phi} = \frac{r}{\sqrt{R_1^2 - r^2}},
\end{aligned} \tag{6}$$

inside the concealment, where $r \leq R_1$ and $r \geq r_0 > 0$. Simulations by the GL EM modeling show that the EM wavefield excited by sources inside the concealment with metamaterial $[D_{GN}]$ in (6) will propagate from the concealment to free space through the single layer cloak. Therefore, the double layer cloak is necessary for sufficient invisibility cloaking.

III. 3D GLOBAL AND LOCAL EM MODELING

In this section, 3D EM integral equations are presented briefly. Based on the integral equations, we propose a 3D Global and Local EM field modeling.

A. 3D ELECTROMAGNETIC INTEGRAL EQUATION

The 3D EM integral equations in frequency domain have been proposed in early papers [1] and [2]. In this paper, we present the EM integral equations in time domain. The integral equations can be derived from Maxwell's equations for the electric and magnetic fields, $E(r, t)$ and $H(r, t)$:

$$\begin{aligned}
\begin{bmatrix} E(r, t) \\ H(r, t) \end{bmatrix} &= \begin{bmatrix} E_b(r, t) \\ H_b(r, t) \end{bmatrix} \\
&+ \int_{\Omega} G_{E,H}^{J,M}(r', r, t) *_t \delta [D(r')] \begin{bmatrix} E_b(r', t) \\ H_b(r', t) \end{bmatrix} dr',
\end{aligned} \tag{7}$$

and

$$\begin{aligned} \begin{bmatrix} E(r, t) \\ H(r, t) \end{bmatrix} &= \begin{bmatrix} E_b(r, t) \\ H_b(r, t) \end{bmatrix} \\ + \int_{\Omega} G_{E,H,b}^{J,M}(r', r, t) *_t \delta[D(r')] &\begin{bmatrix} E(r', t) \\ H(r', t) \end{bmatrix} dr'. \end{aligned} \quad (8)$$

In these equations, E and H are the total electric and magnetic fields in a given medium with prescribed EM sources; E_b and H_b are the fields in a background or reference medium with the same sources (the background fields are also called ‘‘incident’’ fields); and $G_{E,H,b}^{J,M}$ in equation (8) is the EM Green’s tensor for the background medium,

$$G_{E,H,b}^{J,M}(r', r, t) = \begin{bmatrix} E_b^J(r', r, t) & E_b^M(r', r, t) \\ H_b^J(r', r, t) & H_b^M(r', r, t) \end{bmatrix}. \quad (9)$$

The fields E , H , E_b , and H_b are all vector quantities. The elements of the partitioned Green’s tensor are 3×3 tensors (matrices). For example, a point electric current source J in the background medium produces the electric field E_b^J , while a point magnetic source M produces the electric field E_b^M . Similar interpretations hold for H_b^J and H_b^M . Also, $\delta[D]$ is the electromagnetic material parameter variation matrix,

$$\begin{aligned} \delta[D] &= \begin{bmatrix} \delta D_{11} & 0 \\ 0 & \delta D_{22} \end{bmatrix}, \\ \delta D_{11} &= (\bar{\sigma}(r) - \sigma_b I) + (\bar{\varepsilon}(r) - \varepsilon_b I) \frac{\partial}{\partial t}, \\ \delta D_{22} &= (\bar{\mu}(r) - \mu_b I) \frac{\partial}{\partial t}, \end{aligned} \quad (10)$$

δD_{11} and δD_{22} are a 3×3 symmetry, inhomogeneous diagonal matrix for the isotropic material, for anisotropic material, they are an inhomogeneous diagonal or full matrix, I is a 3×3 unit matrix; $\bar{\sigma}(r)$ is the conductivity tensor, $\bar{\varepsilon}(r)$ is the dielectric tensor, $\bar{\mu}(r)$ is susceptibility tensor of the full medium, which can be dispersive (i.e., its properties can depend on the angular frequency ω); σ_b is the conductivity, ε_b is the permittivity, μ_b is the permeability in the background medium; Ω is the finite domain in which the parameter variation matrix $\delta[D] \neq 0$; the $(\bar{\varepsilon}(r) - \varepsilon_b I)E$ is the induced electric polarization; and $(\bar{\mu}(r) - \mu_b I)H$ is the induced magnetization. Finally, $*_t$ is convolution with respect to time, t .

B. 3D GL EM MODELING

Although the two integral equations (7) and (8) are equivalent, there are numerical advantages in using both sets simultaneously. Based on the integral equation, the GL EM modeling in the time domain is proposed in this section. The 3D GL EM modeling and integral equations in the frequency domain have been developed in early papers [1-2].

(3.1) The domain Ω is divided into a set of N sub domains, $\{\Omega_k\}$, such that $\Omega = \bigcup_{k=1}^N \Omega_k$. The division can be mesh or meshless.

(3.2) When $k = 0$, let $E_0(r, t)$ and $H_0(r, t)$ are the analytical global field, $E_0^J(r', r, t)$, $H_0^J(r', r, t)$, $E_0^M(r', r, t)$, and $H_0^M(r', r, t)$ are the analytical global Green’s tensor in the background medium. By induction, suppose that $E_{k-1}(r, t)$, $H_{k-1}(r, t)$, $E_{k-1}^J(r', r, t)$, $H_{k-1}^J(r', r, t)$, $E_{k-1}^M(r', r, t)$, and $H_{k-1}^M(r', r, t)$ are calculated in the $(k-1)^{th}$ step in the subdomain Ω_{k-1} .

(3.3) In $\{\Omega_k\}$, upon substituting $E_{k-1}(r, t)$, $H_{k-1}(r, t)$, $E_{k-1}^J(r', r, t)$, $H_{k-1}^J(r', r, t)$, $E_{k-1}^M(r', r, t)$, and $H_{k-1}^M(r', r, t)$ into the integral equation (8), the EM Green’s tensor integral equation (8) in Ω_k is reduced into 6×6 matrix equations. By solving the 6×6 matrix equations, we obtain the Green’s tensor field $E_k^J(r', r, t)$, $H_k^J(r', r, t)$, $E_k^M(r', r, t)$, and $H_k^M(r', r, t)$.

(3.4) According to the integral equation (7), the electromagnetic field $E_k(r, t)$ and $H_k(r, t)$ are updated by the interactive scattering field between the Green’s tensor and local polarization and magnetization in the subdomain Ω_k as follows,

$$\begin{aligned} \begin{bmatrix} E_k(r, t) \\ H_k(r, t) \end{bmatrix} &= \begin{bmatrix} E_{k-1}(r, t) \\ H_{k-1}(r, t) \end{bmatrix} \\ + \int_{\Omega_k} &\left\{ \begin{bmatrix} E_k^J(r', r, t) & H_k^J(r', r, t) \\ E_k^M(r', r, t) & H_k^M(r', r, t) \end{bmatrix} \right. \\ &*_t \delta[D(r')] \begin{bmatrix} E_{k-1}(r', t) \\ H_{k-1}(r', t) \end{bmatrix} \left. \right\} dr' \end{aligned} \quad (11)$$

(3.5) The steps (3.2) and (3.4) form a finite iteration, $k = 1, 2, \dots, N$, the $E_N(r, t)$ and $H_N(r, t)$ are the electromagnetic field of the GL modeling method. The GL electromagnetic field modeling in the time space domain is short named as GLT method.

The GL EM modeling in the space frequency domain is proposed in the paper [2], we call the GL modeling in frequency domain as GLF method.

IV. INTERACTION BETWEEN THE EM WAVE FIELD WITH CLOAKS

A. Theoretical Analysis Of Interaction Between The EM Wave Field With The GL Double Layer Cloaks

Theoretical analysis of the interaction between the EM wave with GL cloaks are presented in this section.

Statement 1: Let domain Ω_{GL} , equation (3), and anisotropic metamaterial D_{GL} , equation (4), be a ‘‘GL’’ double layer cloak, and let the concealed central sphere $|\vec{r}| < R_1$ and the region outside the cloak $|\vec{r}| > R_3$ be filled with a normal electromagnetic material with permittivity and permeability, $\varepsilon = \varepsilon_b$, $\mu = \mu_b$. We claim the following: (1) provide EM wavefield is excited by sources located inside the concealment of GL cloak, $|\vec{r}_s| < R_1$, the EM wavefield never be disturbed by the cloak; (2) provide EM wavefield is excited by sources located inside concealment or the inner layer of the cloak, $|\vec{r}_s| < R_2$, the EM wavefield is absorbed in the inner layer Ω_I and

does not extend outside the boundary $r = R_2$. (3) provide the wavefield is excited by sources located outside of the cloak, $|\vec{r}'_s| > R_3$, the EM wavefield propagates as if in free space, undisturbed by the cloak; (4) provide the EM wavefield is excited by sources outside cloak or inside outer layer, $|\vec{r}'_s| > R_2$, the EM wavefield does not penetrate into the inner layer and the concealed region, $|\vec{r}'| < R_2$.

B. No Maxwell EM Wavefield Can Be Excited By Nonzero Local Sources Inside The Single Layer Cloaked Concealment Filled With Normal Materials

Statement 2: Suppose that a 3D anisotropic inhomogeneous single layer cloak domain separates the whole space into three sub domains: one is the single layer cloak domain Ω_{clk} with the cloaking material; another is the cloaked concealment domain Ω_{conl} with normal EM materials; and the third is free space outside the cloak. If the Maxwell EM wavefield excited by a point source or local sources outside the concealment Ω_{conl} vanishes inside the concealment Ω_{conl} , then there is no Maxwell EM wave field excited by the local sources inside the cloaked concealment Ω_{conl} .

The Maxwell EM wavefield is an EM wave field that satisfies the Maxwell equation and appropriate interface boundary conditions. We use an inverse process to prove the *statement 2* as follows: Suppose that there exists a Maxwell EM wavefield excited by the local sources inside the concealment, filled with the normal materials, the wavefield will satisfy the Maxwell equation in all of the space, including in the anisotropic inhomogeneous cloaking layer Ω_{clk} and in the concealment, Ω_{conl} ; and also satisfies boundary conditions on the interfaces, S_1 and S_2 . S_1 is the interface boundary between the cloaking region Ω_{clk} and the concealment domain Ω_{conl} , and also is the inner boundary surface of the cloaking domain Ω_{clk} . S_2 is the interface boundary between the cloaking region Ω_{clk} and free space outside; it also is the outer boundary surface of the cloaking region Ω_{clk} .

Let $R_c = R^3 - \Omega_{clk} \cup \Omega_{conl}$, $R_d = R^3 - \Omega_{conl}$, and by integral equation (7), the EM wave field satisfies

$$\begin{bmatrix} E(r, t) \\ H(r, t) \end{bmatrix} = \begin{bmatrix} E_b(r, t) \\ H_b(r, t) \end{bmatrix} + \int_{\Omega_{clk} \cup \Omega_{conl}} G_{E,H}^{J,M}(r', r, t) *_t \delta[D] \begin{bmatrix} E_b(r', t) \\ H_b(r', t) \end{bmatrix} dr', \quad (12)$$

where $G_{E,H}^{J,M}(r', r, t)$ is the Green's tensor, its components E^J , H^J , E^M , and $H^M(r', r, t)$ are the Green's function on $\Omega_{clk} \cup \Omega_{conl} \cup R_c$, excited by the point impulse sources outside the concealment, $r \in R_d$. By the assumptions, $G_{E,H}^{J,M}(r', r, t)$ exists on $\Omega_{clk} \cup \Omega_{conl} \cup R_c$ and when $r' \in \Omega_{conl}$, $G_{E,H}^{J,M}(r', r, t) = 0$. The integral equation (12)

becomes to

$$\begin{bmatrix} E(r, t) \\ H(r, t) \end{bmatrix} = \begin{bmatrix} E_b(r, t) \\ H_b(r, t) \end{bmatrix} + \int_{\Omega_{clk}} G_{E,H}^{J,M}(r', r, t) *_t \delta[D] \begin{bmatrix} E_b(r', t) \\ H_b(r', t) \end{bmatrix} dr'. \quad (13)$$

Consider the Maxwell equation in R_d , the virtual source is located r , $r \in R_d$ and the point source is located r_s , the variable in the following equations is r' , $r_s \in \Omega_{conl}$ and $r_s \notin R_d$, we have

$$\begin{bmatrix} -\nabla \times & \nabla \times \\ -\nabla \times & \nabla \times \end{bmatrix} G_{E,H}^{J,M}(r', r, t) = [D] G_{E,H}^{J,M}(r', r, t) + I\delta(r', r)\delta(t), \quad (14)$$

and

$$\begin{bmatrix} -\nabla \times & \nabla \times \\ -\nabla \times & \nabla \times \end{bmatrix} \begin{bmatrix} E_b \\ H_b \end{bmatrix}(r', r_s, t) = [D_b] \begin{bmatrix} E_b \\ H_b \end{bmatrix}(r', r_s, t), \quad (15)$$

Convolving equation (14) with $[E_b(r', t), H_b(r', t)]$, and equation (15) with $G_{E,H}^{J,M}(r', r, t)$, subtracting the second result from the first, integrating by parts, and making some manipulations gives

$$\begin{bmatrix} E_b(r, t) \\ H_b(r, t) \end{bmatrix} + \int_{\Omega_{clk}} G_{E,H}^{J,M}(r', r, t) *_t \delta[D] \begin{bmatrix} E_b(r', t) \\ H_b(r', t) \end{bmatrix} dr' = \oint_{S_1} G_{E,H}^{J,M}(r', r, t) \otimes_t \begin{bmatrix} E_b(r', t) \\ H_b(r', t) \end{bmatrix} d\vec{S}, \quad (16)$$

where \otimes_t is cross convolution. From the assumption of the *statement 2* that "the Maxwell EM wavefield excited by a point source or local sources outside the concealment Ω_{conl} vanishes inside the concealment Ω_{conl} ", and virtual source r is located outside the concealment, $r \in R_d$, if $r' \in \Omega_{conl}$, $G_{E,H}^{J,M}(r', r, t) = 0$. By continuity, when $r' \in S_1$, we have $G_{E,H}^{J,M}(r', r, t) = 0$. Continuity of $G_{E,H}^{J,M}(r', r, t)$ at interface implies that the term in right hand side of (16) vanishes, giving

$$\begin{bmatrix} E_b(r, t) \\ H_b(r, t) \end{bmatrix} + \int_{\Omega_{clk}} G_{E,H}^{J,M}(r', r, t) *_t \delta[D] \begin{bmatrix} E_b(r', t) \\ H_b(r', t) \end{bmatrix} dr' = 0. \quad (17)$$

Substituting equation (17) into the integral equation (13) gives

$$\begin{bmatrix} E(r, t) \\ H(r, t) \end{bmatrix} = 0. \quad (18)$$

From continuity condition on the EM wave field, we obtain the following over vanishing condition on the boundary S_1 of the concealment Ω_{conl} ,

$$\left[\begin{array}{c} E(r, r_s, t) \\ H(r, r_s, t) \end{array} \right] \Big|_{S_1} = 0, \quad (19)$$

where r_s denotes point source location inside of the concealment, r is EM field receiver point, $r \in S_1$. Because the EM wavefield is excited by local sources inside of the concealment domain Ω_{conl} , it satisfies the following Maxwell equation with variable r' ,

$$\begin{aligned} & \left[\begin{array}{c} \nabla \times \\ -\nabla \times \end{array} \right] \left[\begin{array}{c} E \\ H \end{array} \right] (r', r_s, t) \\ &= [D_{conl}] \left[\begin{array}{c} E \\ H \end{array} \right] (r', r_s, t) + Q(r', r_s, t). \end{aligned} \quad (20)$$

where $[D_{conl}] = \text{diag}[\varepsilon_r \varepsilon_0 I, \mu_r \mu_0 I](\partial/\partial t)$ with the normal EM material parameters, $\varepsilon_r \geq 1$ and $\mu_r \geq 1$ are relative EM parameters, ε_0 is basic permittivity and μ_0 is basic permeability, I is 3×3 unit matrix, $r_s \in \Omega_{conl}$ is the local source location, $Q(r', r_s, t)$ is the nonzero local source inside the concealment, Ω_{conl} . Let $G_{E,H,conl}^{J,M}(r', r, t)$ be *Greens* tensor which satisfies

$$\begin{aligned} & \left[\begin{array}{c} 0 \quad \nabla \times \\ -\nabla \times \quad 0 \end{array} \right] G_{E,H,conl}^{J,M}(r', r, t) \\ &= [D_{conl}] G_{E,H,conl}^{I,M}(r', r, t) \\ &+ I \delta(r', r) \delta(t) \end{aligned} \quad (21)$$

Convolving $[E(r', t), H(r', t)]$ with (21), and $G_{E,H,conl}^{J,M}(r', r, t)$ with (20), subtracting the second result from the first, taking the integral to Ω_{conl} , and use integration by parts and other manipulations, we have

$$\begin{aligned} & \left[\begin{array}{c} E(r, r_s, t) \\ H(r, r_s, t) \end{array} \right] \\ &= \int_{\Omega_{conl}} G_{E,H,conl}^{J,M}(r', r, t) *_t Q(r', r_s, t) dr' \\ &+ \oint_{\partial\Omega_{conl}} G_{E,H,conl}^{J,M}(r', r, t) \otimes_t \left[\begin{array}{c} E(r', r_s, t) \\ H(r', r_s, t) \end{array} \right] dr', \end{aligned} \quad (22)$$

\otimes_t denotes the cross convolution, and $\partial\Omega_{conl} = S_1$. Because of the over vanishing condition (19),

$$\left[\begin{array}{c} E(r, r_s, t) \\ H(r, r_s, t) \end{array} \right] \Big|_{S_1} = 0,$$

we have

$$\begin{aligned} & \left[\begin{array}{c} E(r, r_s, t) \\ H(r, r_s, t) \end{array} \right] = \\ &= \int_{\Omega_{conl}} G_{E,H,conl}^{J,M}(r', r, t) *_t Q(r', r_s, t) dr'. \end{aligned} \quad (23)$$

Because $G_{E,H,conl}^{J,M}(r', r, t) \neq 0$ and $Q(r', r_s, t) \neq 0$, so,

$$\left[\begin{array}{c} E(r, r_s, t) \\ H(r, r_s, t) \end{array} \right] \neq 0. \quad (24)$$

From the continuity of the EM wavefield, the nonzero EM wave field (24) results that

$$\left[\begin{array}{c} E(r, r_s, t) \\ H(r, r_s, t) \end{array} \right] \Big|_{S_1} \neq 0. \quad (25)$$

The EM wavefield is nonzero on the boundary S_1 in (25) that is an obvious contradiction with the same EM wavefield is zero on the boundary S_1 in (19). Therefore, we proved statement 2. Result (24) can also be derived more simply and obvious from the integral expression (23). Let the source be a point impulse current source with polarization direction \vec{x} , i.e.,

$$Q(r, r_s, t) = \delta(r - r_s) \delta(t) \vec{x}. \quad (26)$$

Substituting (26) and $\varepsilon_r = 1.0$ and $\mu_r = 1.0$ into the (23), gives

$$\left[\begin{array}{c} E(r, r_s, t) \\ H(r, r_s, t) \end{array} \right] = \left[\begin{array}{c} E_x^J(r, r_s, t) \\ H_x^J(r, r_s, t) \end{array} \right] \quad (27)$$

$$E_x^J(r, r_s, t) = \left[\begin{array}{c} E_{xx}(r, r_s, t) \\ E_{xy}(r, r_s, t) \\ E_{xz}(r, r_s, t) \end{array} \right] \quad (28)$$

$$\begin{aligned} & E_{xx}(r, r_s, t) \\ &= -\frac{1}{8\pi^2 \varepsilon} \frac{\partial^2}{\partial x^2} \frac{\delta(t - \sqrt{\varepsilon \mu} |r - r_s|)}{|r - r_s|} \\ &+ \frac{1}{8\pi^2 \mu} \frac{\partial^2}{\partial t^2} \frac{\delta(t - \sqrt{\varepsilon \mu} |r - r_s|)}{|r - r_s|} \end{aligned} \quad (29)$$

It is obvious that when $r \in S_1$

$$E_{xx}(r, r_s, t)|_{r \in S_1} \neq 0. \quad (30)$$

The electric intensity field $E_{xx}(r, r_s, t)|_{r \in S_1} \neq 0$ in (30) and $E_{xx}(r, r_s, t)|_{r \in S_1} = 0$ in (19) are an obvious contradiction. The *Statement 2* is true.

V. SIMULATIONS OF THE EM WAVE FIELD THROUGH THE DOUBLE LAYER CLOAK

A. The Model of The Double Layer Cloak

The full 3D simulation model is a unit cube, $[0.5, 0.5]^3$, centered on the origin, discretized on a 201^3 mesh, with uniform mesh spacing of $0.005m$. The EM wavefield is excited by a point electric source:

$$s(r, r_s, t) = \delta(r - r_s) \delta(t) \vec{e}, \quad (31)$$

at location r_s where \vec{e} is the (unit) polarization vector. the time step $dt = 0.3333 \times 10^{-10}$; the frequency band is from $0.05GHz$ to $15GHz$. The shortest wavelength is about $0.02m$. The GL double layer EM cloak consists of inner and outer annular regions, $\Omega_{GL} = \Omega_I \cup \Omega_O$,

equation (3), with centers at the origin, which is situated by proposed anisotropic metamaterial D_{GL} , equation (4), the concealed central sphere $|\vec{r}| < R_1$ and the region outside the cloak $|\vec{r}| > R_3$ is filled with a normal electromagnetic material with basic permittivity and permeability, $\varepsilon = \varepsilon_b, \mu = \mu_b$. The inner boundary of the cloak is $R_1 = 0.2m$; the middle shell boundary between the two layers is $R_2 = 0.3m$; and the outer boundary is $R_3 = 0.45m$. In the simulations, the sphere region $r \leq R_3$ is actually modeled in spherical coordinates, (r, θ, ϕ) , where θ is polar angle. The sphere is divided 180^3 cells. The spherical coordinate grid is superimposed on the rectangular grid used to mesh the domain outside shell $r = R_3$. Because the cloaking materials are radial dependent, the EM modeling is reduced to the system of the one dimensional GL modeling by using the sphere harmonic expansion.

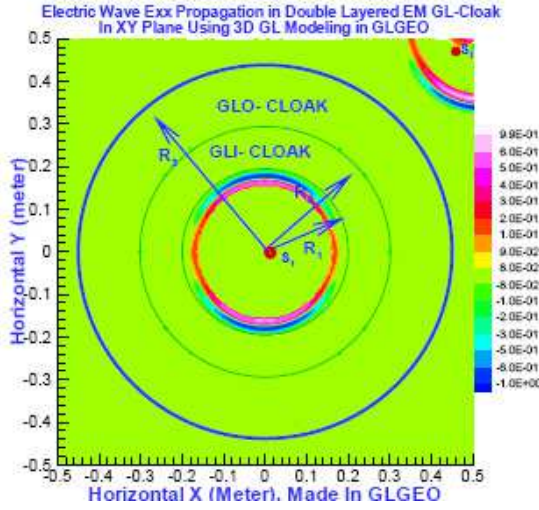


FIG. 1: (color online) At time step $18dt$, the wave front of the *First electric wave*, $E_{xx,1}$, propagates inside the concealment $r < R_1$. The front of *Second EM wave*, $E_{xx,2}$, is located in free space, the right and top corner outside of the whole GL double layer cloak.

B. Simulation I

In this subsection, the simulation I is presented that an inner point source in the concealment and other outer source in the free space are used to excite the EM wave propagation through the double layer cloak. The point impulse current source with polarization direction \vec{x} , i.e.

$$S(r, r_s, t) = \delta(r - r_s) \delta(t) \vec{x}. \quad (32)$$

The first point current source is located inside the concealment at $(0.0012m, 0.0m, 0.0m)$, by which the excited EM wave is named as *First EM wave*, its component $E_{xx,1}$ is labeled *First electric wave*. The second current point source is located in free space at

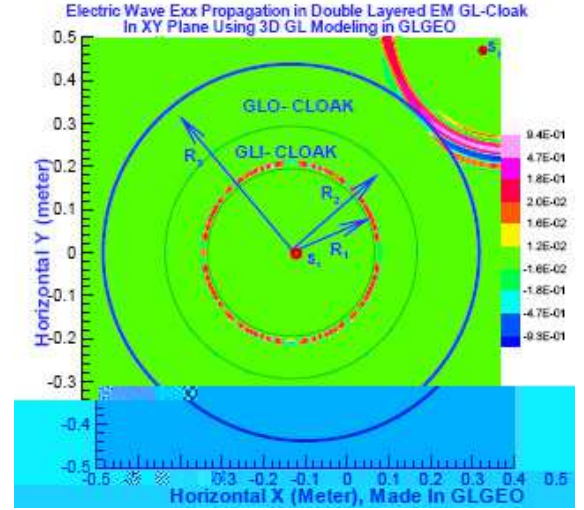


FIG. 2: (color online) At this moment of the time step $30dt$, the front of the *First electric wave*, $E_{xx,1}$, propagates enter to the inner layer, $R_1 \leq r \leq R_2$; the front of *Second electric wave*, $E_{xx,2}$, reaches the outer boundary $r = R_3$ of the GL double layer cloak.

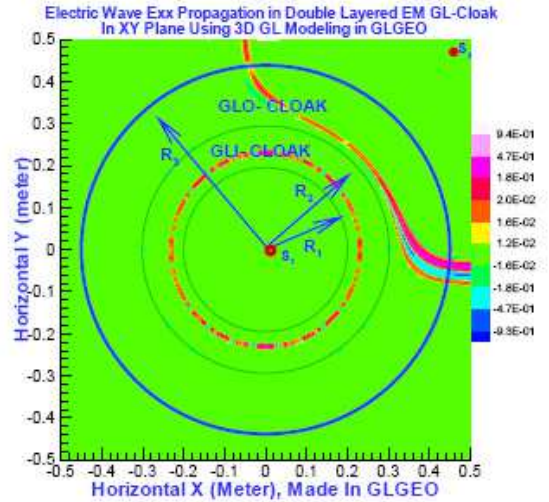


FIG. 3: (color online) At the time step $58dt$, the *First electric wave*, $E_{xx,1}$, is propagating inside the inner layer, $R_1 \leq r \leq R_2$, and becomes very slow. The part of the front of *Second electric wave*, $E_{xx,2}$, has been inside of outer layer, $R_2 \leq r \leq R_3$, and being backward bending

$(0.518m, 0.518m, 0.0)$ where is in the right and top corner outside the double layer cloak. The EM wave by the second source is named as *Second EM wave*. Its component $E_{xx,2}$, is labeled *Second electric wave*. Figure 1-6 show a series of snapshots of an EM field propagating in and around the double layer cloak. The Figure 1 shows that at time step $18dt$, the wave front of the *First electric wave*, $E_{xx,1}$, propagates inside the central sphere concealment $r < R_1$ and never be disturbed by the inner layer; The front of *Second EM wave*, $E_{xx,2}$,

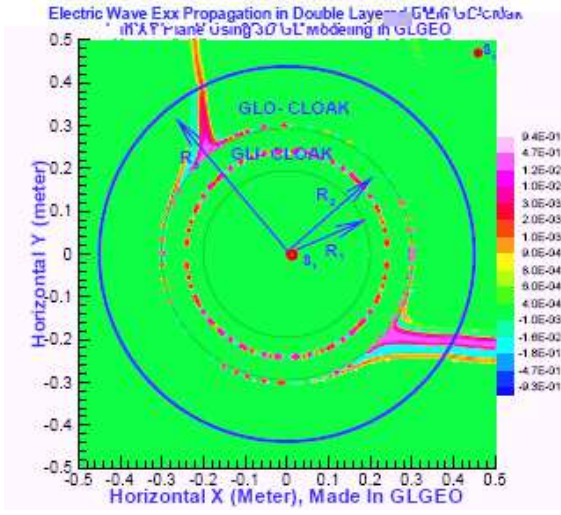


FIG. 4: (color online) At time step $75dt$, the *Second electric wave*, $E_{xx,2}$, is propagating inside of the outer layer, $R_2 \leq r \leq R_3$, and around the shell $r = R_2$ and never penetrate into inner layer and concealment, $r < R_2$. It does split into the two phases around the shell $r = R_2$. The *First electric wave*, $E_{xx,1}$, is propagating inside the inner layer, $R_1 \leq r \leq R_2$.

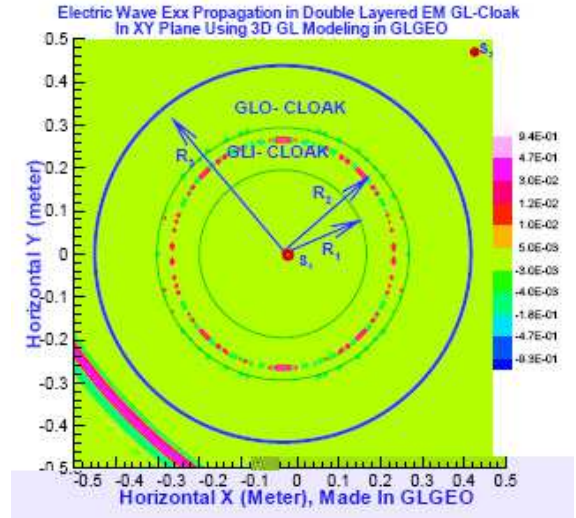


FIG. 6: (color online) At time step $128dt$, the *Second electric wave*, $E_{xx,2}$ has propagated outside the GL double layer cloak, a small part of its wave front is located in the left and low corner of the plot frame, which never be disturbed. The *First electric wave*, $E_{xx,1}$, is still propagating inside the inner layer, $R_1 \leq r \leq R_2$.

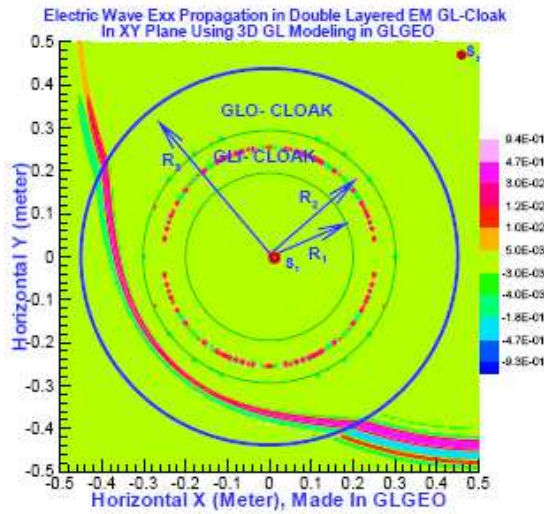


FIG. 5: (color online) At time step $98dt$, one part of front the *Second electric wave*, $E_{xx,2}$, is propagating inside of the outer layer, $R_2 \leq r \leq R_3$, and around to other side far source. It is a little forward bending. The *First electric wave*, $E_{xx,1}$, is still propagating inside the inner layer, $R_1 \leq r \leq R_2$.

is located in free space, the right and top corner outside the double layer cloak. At the moment $30dt$ in Figure 2, the front of the *First electric wave*, $E_{xx,1}$, propagates enter to the inner layer, $R_1 \leq r \leq R_2$; The front of *Second electric wave*, $E_{xx,2}$, reaches the outer shell boundary $r = R_3$ of the cloak and never be disturbed. At the time step $58dt$, the *First electric wave*, $E_{xx,1}$, is propagating inside the inner layer, $R_1 \leq r \leq$

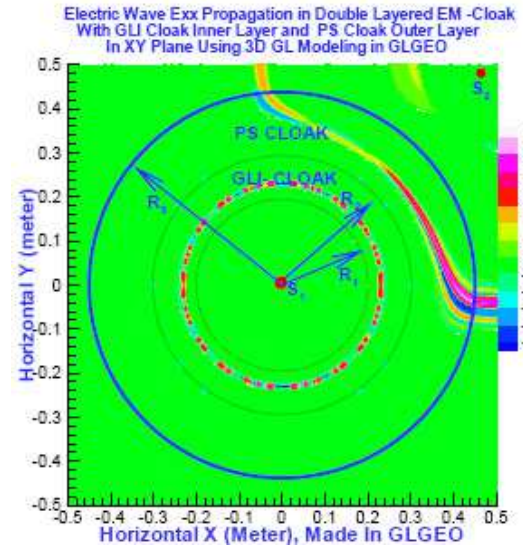


FIG. 7: (color online) In the double layer cloak, inner layer is situated with GLI cloak material in (1), outer layer is filled with PS cloak material. At the time step $58dt$, the *First electric wave*, $E_{xx,1}$, is propagating inside inner layer; The *Second electric wave* propagates inside outer layer with more backward bending and more slow than EM wavefield in GLO material (2) in Figure 5.

R_2 , and becomes very slow; The part of the front of *Second electric wave*, $E_{xx,2}$, propagates inside outer layer, $R_2 \leq r \leq R_3$, and being backward bending. The EM wave propagation image snapshot is presented in Figure 3. In the Figure 4, at time step $75dt$, the

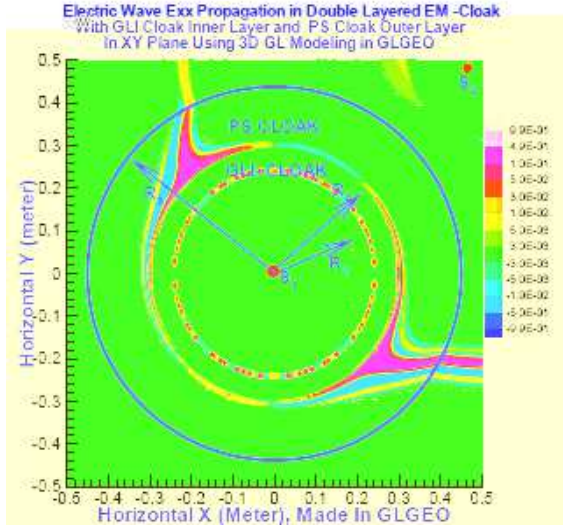


FIG. 8: (color online) In the double layer cloak GLPS arranged in Figure 7, at the time step $75dt$, the *First electric wave*, $E_{xx,1}$, is propagating inside inner layer; The *Second electric wave* propagates around the shell $r = R_2$ with more forward bending than EM wavefield in GLO material (2) in Figure 5.

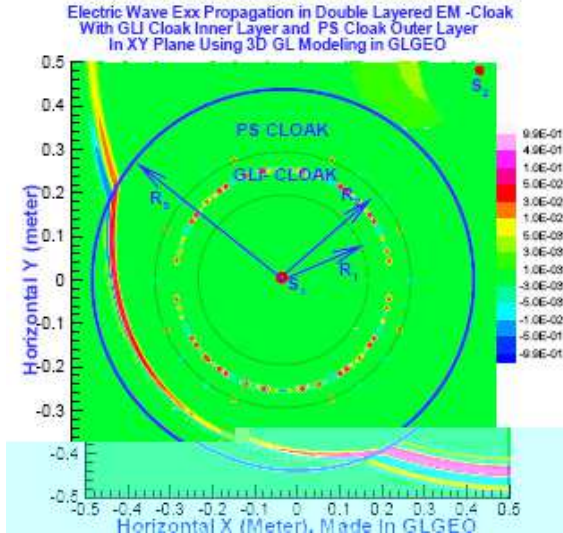


FIG. 9: (color online) In the double layer cloak GLPS in Figure 7, at the time step $98dt$, the *First electric wave*, $E_{xx,1}$, is propagating inside inner layer; The *Second electric wave* propagates inside outer layer around to side far source with more forward bending and more fast than EM wavefield does in GLO material (2) in Figure 5.

First electric wave, $E_{xx,1}$, is still propagating inside the inner layer, $R_1 \leq r \leq R_2$; The *Second electric wave*, $E_{xx,2}$, is propagating inside the outer layer cloak, $R_2 \leq r \leq R_3$, and around the shell $r = R_2$ and never penetrate into the inner layer and concealment, $r \leq R_2$. It does split into the two phases around the shell $r = R_2$, the

front phase speed exceeds the light speed; the back phase is slower than the light speed. In the figure 5, at time step $98dt$, one part of front the *Second electric wave*, $E_{xx,2}$, is propagating inside the outer layer, $R_2 \leq r \leq R_3$. has a little forward bending and never penetrate into the inner layer and the concealment, i.e. $r \leq R_2$. The *First electric wave*, $E_{xx,1}$, is still propagating inside of the inner layer, $R_1 \leq r \leq R_2$. At time step $128dt$, the *Second electric wave*, $E_{xx,2}$ has propagated outside double layer cloak, a small part of its wave front is located in the left and low corner of the plot frame which is shown in the Figure 6, most part of front of the $E_{xx,2}$ electric wave field has been out of the plot frame The exterior EM wave outside the cloak never been disturbed by the cloak and never penetrate enter its concealment and inner layer. At same time step, the *First electric wave*, $E_{xx,1}$, is still propagating inside the the inner layer, $R_1 \leq r \leq R_2$. It can be very closed to the interface boundary shell $r = R_2$, However, it can not be reached to the boundary $r = R_2$ for any long time. That means that the interior EM wavefield excited by source inside the concealment is complete absorbed by the inner layer. The inner layer metamaterial, in equation (1), cloaks outer space from the local field excited in the inner layer and concealment, which can also be useful for making a complete absorption boundary condition to truncate infinite domain in numerical simulation.

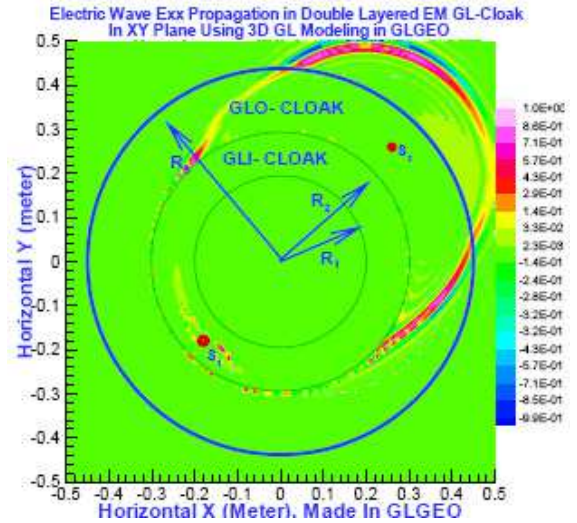


FIG. 10: (color online) At time step $30dt$, one part of the front of the *Second electric wavefield*, $E_{xx,2}$, propagates in free space with disturbance, its other part of the front has been propagating around the shell $r = R_2$; It does not propagate into the inner layer and concealment. The *First electric wave*, $E_{xx,1}$, is very slow and just starts to propagate in the inner layer.

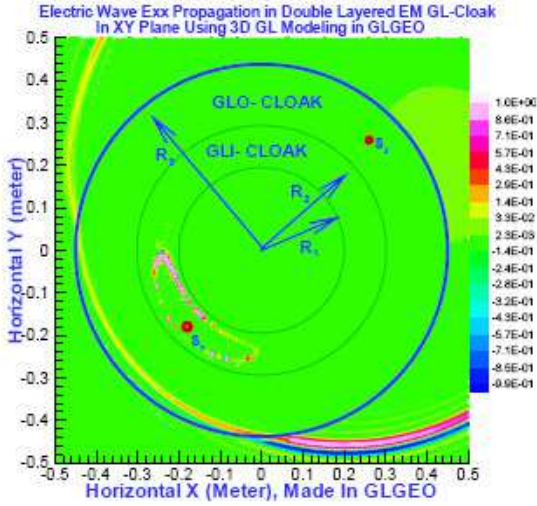


FIG. 11: (color online) At time step $68dt$, front of the *First electric wave*, $E_{xx,1}$, is very slow propagating inside inner layer $R_1 < r < R_2$; The most part of front of *Second EM wave*, $E_{xx,2}$, propagates in free space with disturbance, its other small part of front propagates in the outer layer around to side far source, but it does not propagate into the inner layer.

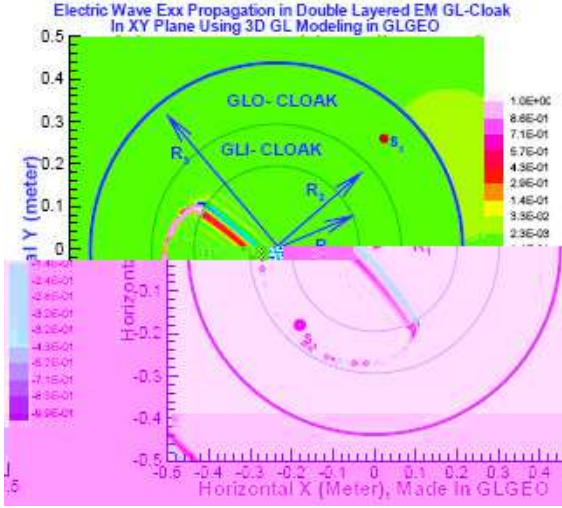


FIG. 12: (color online) At moment $98dt$, one part of the front of the *First electric wave*, $E_{xx,1}$, propagates enter to the concealment; other part of the front is still propagating inside of inner layer, $R_1 \leq r \leq R_2$, it does not propagate outside shell $r = R_2$; The front of *Second electric wave*, $E_{xx,2}$, has propagated outside all cloak, only very small part of the front is located the left lower corner of the figure frame.

C. Simulation II

To compare the properties between the GLO cloak and PS cloak, we use PS cloak [4] as outer layer and GLI cloak, in equation (1), as inner layer to construct a GLPS double layer cloak. The simulations of the EM

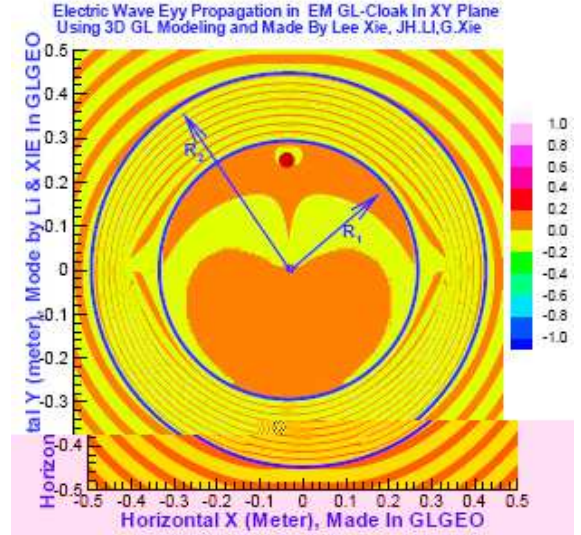


FIG. 13: (color online) The PS single layer cloaked concealment is filled with a permittivity single negative metamaterial, The electric wavefield E_{xx} excited by a point source inside the concealment propagates out to free space through the cloak.

wavefield propagation through the GLPS cloak is presented in simulation II. The cloak geometry and mesh configuration is described in subsection A. Because the GLI cloak, in equation (1), is used as inner cloak of GL double layer cloak and GLPS double layer cloak, the *First electric wave* propagation in timestep $30dt$, $58dt$, and $98dt$ are as same as in Figure 3 and Figure 7; Figure 4 and Figure 8, Figure 5 and Figure 9, respectively. At timesep $58dt$, the *Second electric wave*, $E_{xx,2}$, propagating in PS cloak is more slow and more backward bending than the field does in GLO outer layer, in Figure 3. At timestep $75dt$, the front of *Second electric wave*, $E_{xx,2}$, propagating in outer layer of GL cloak in Figure 4, is better than the field propagation in PS cloak, in Figure 8. In particular, at timestep $98dt$, *Second electric wave*, $E_{xx,2}$, propagating in layer PS cloak has more foeward bending in Figure 9, but the field has a little forward bending in GLO outer layer in figure 4. Summary, GLO cloak material degeneration is weaker and better than the PS cloak.

D. Simulation III

The EM wavefield excited by a point source inside the inner layer and other point source inside the outer layer of GL cloak propagates through the double layer cloak that is presented in this subsection. By the first point current source at $(-0.18m, -0.18m, 0.0)$, the excited EM wavefield $E_{xx,1}$ is labeled *First electric wave*. The second current point source at $(0.258m, 0.258m, 0.0)$ excites the EM wavefield, $E_{xx,2}$, which is labeled *Second electric wave*. The Figure 10 shows that

at time step $30dt$, one part of the front of the *Second electric wavefield*, $E_{xx,2}$, propagates in free space with disturbance in [15], its other part of the front has been propagating around the shell $r = R_2$; It does not propagate into the inner layer and concealment. The *First electric wave*, $E_{xx,1}$, is very slow and just starts to propagate in the inner layer. In the Figure 11, at time step $68dt$, front of the *First electric wave*, $E_{xx,1}$, is very slow propagating inside inner layer $R_1 < r < R_2$; The most part of front of *Second EM wave*, $E_{xx,2}$, propagates in free space with disturbance, its other part of front propagates inside the outer layer around to side far source, but it does not propagate into the inner layer. The wavefield propagating at moment $98dt$ is presented in figure 12. One part of the front of the *First electric wave*, $E_{xx,1}$, propagates enter to the concealment; other part of the front is still propagating inside of inner layer, $R_1 \leq r \leq R_2$, it does not propagate outside shell $r = R_2$; The front of *Second electric wave*, $E_{xx,2}$, has propagated outside all cloak, only very small part of the front is located the left lower corner of the figure frame

E. Simulation IV

For studying the EM wavefield excited by source inside a concealment which is cloaked by a single layer cloak, we propose and situate a novel negative dielectric and positive susceptibility metamaterial $[D]_{GN}$, in equation (6), inside the concealment, where $r \leq R_1$ and $r \geq r_0 > 0$. The concealment is cloaked by the PS cloak [4], in equation (5). The simulation domain and mesh configuration is described in subsection A. A time harmonic point source with polarization in y direction and frequency $0.57 \times 10^{10} Hz$,

$$s(r, r_s, t) = \delta(r - r_s)e^{i\omega t}\vec{y}, \quad (33)$$

is located in the point r_s , $(0.0, 0.26, 0.0)$. Simulations by the GL EM modeling show that, in Figure 13, the EM wavefield E_{yy} excited by the source in (33) inside the concealment filled with the metamaterial is propagating from the concealment to free space through the PS single layer cloak. Therefore, the double layer cloak is necessary for sufficient invisibility cloaking. This single negative refraction metamaterial, in equation (6), will be investigated and detailed presented in next paper.

VI. ADVANTAGES

A. The EM GL Double Layer Cloak Is Robust and Sufficient For Invisibility

The figure 10-12 clearly show that at moment of the $30dt$, $68dt$, and $98dt$ time step, the wave front of the Second electric wave has propagated outside the cloak and go to free space with disturbance. The result reminds us that if only single outer layer cloak Ω_O , or PS cloak is adopted, and there is a little crack loss on the inner side of the boundary surface $\partial\Omega_{O-}$, some EM or current source inside the Ω_O will excite the EM wave propagation go out to free space and expose the cloak immediately. Moreover, the Figure 13 shows that the EM wavefield E_{yy} excited by the source in (33) inside the concealment filled with the metamaterial is propagating from the concealment to free space through the PS single layer cloak. Such that the single layer cloak complete lose the cloaking function. The GL double layer cloak overcomes the weakness that is also shown in the figure 1-12. The wave front of the First electric wave, which is excited by a point source inside the inner layer cloak Ω_I , or inside the concealment, is always propagating inside of inner layer cloak Ω_I or concealment Ω_{conl} and never propagate outside of the interface shell $r = R_2$. Any EM field inside the inner layer or inside the concealment can not be propagated outside the shell $r = R_2$. Therefore, the EM GL double layer cloak is robust and sufficient for invisibility.

Using the GL method theoretical analysis, the statement 2 in section 4 is rigorously proved. It states that "there exists no Maxwell electromagnetic wavefield can be excited by nonzero local sources inside of the single layer cloaked concealment with the normal EM materials". The invisibility of the single layer cloak and existence of Maxwell EM wave field excited by the local sources inside its concealment is inconsistent. Provide only single outer layer cloak is adopted, the EM field excited by local sources inside of its concealment with normal materials does not satisfy the Maxwell equation. The EM chaos phenomena, which is divorced from the Maxwell equation governing, may damage devices and human inside the concealment, or may degrade the invisibility of the cloak. The single layer cloak is not complete and unsafe. The Figure 13 shows when a special metamaterial fills into the concealment, the single layer cloak complete lose cloaking function. The GL double layer cloak in this paper or double coating in paper [8] are necessary for the complete invisibility function. The GL double layer cloak is different from the double coating in paper [8]. The simulations in Figures 1-12 show that the inner layer metamaterial of GL double layer, in equation (1), does not disturb and reflect the EM field excited by sources inside the concealment and does not change the EM environment in the concealment. Therefore, GL cloak is safe metamaterial.

B. Frequency Band And Geometry

Many simulations and theoretical analysis by the GL method show that the idea EM GL double layer cloak is of the invisibility function for all frequencies. However, the practical material has some loss. The frequency band will be depended on the rate of the material loss.

When r is decreasing and going to R_2 in outer layer, the EM wavefield speed in PS cloak, In equation (5), is increasing to infinite with the strong divergent rate $1/(r - R_2)$, but the EM wavefield speed in outer layer of GL cloak, in equation (1), is increasing with the weak divergent rate $1/\sqrt{r - R_2}$. In the side near the source, the simulation in Figure 7 shows that *Second electric wave*, $E_{xx,2}$, propagation is more slow and more backward bending inside the PS cloak than the field does in outer layer of GL cloak in Figure 3. In the side far the source, the simulation in Figure 9 shows that *Second electric wave*, $E_{xx,2}$, propagation is more fast and more forward bending inside the PS cloak than the field does in outer layer of GL cloak in Figure 5.

The comparisons between the EM wave propagation inside the GL cloak and PS cloak, in Figure 3 - 5 and Figure 7 - 9, show that the GL cloak has better properties to reduce the dispersion and degeneration. Therefore, a reasonable frequency band of the GL double layer cloak for low loss rate may be obtained in practical fabrication. The EM GL double layer cloak can be extended to have double ellipsoid annular layer and other double strip geometry or use non euclidean geometry [10] in outer layer cloak and GLI in (1) in inner layer to make wide frequency band double layer cloak in next paper. The experiments in this field, the pioneering demonstration by D. Schurig et al in [11] and the recent paper by R. Liu et al. in [12] may be important help for improving cloak model and simulation. As early in 2001, a double layer cloth phenomenon has been observed in Lawrence Berkely National Laboratory which is published in SEG Expanded Abstracts in 2002 [13]. For studying and simulating the strange phenomenon and metamaterials, we developed the effective GL modeling and inversion. The first paper of the GL method and a relative EM "mirage" phenomenon have been presented in PIERS 2005 and published in the proceeding of PIERS 2005 in Hangzhou in [14] and [15].

C. Advantages Of The GL Method

The GL EM modeling is fully different from FEM and FD and Born approximation methods and overcome their difficulties. There is no big matrix equation to solve in GL method. Moreover, it does not need artificial boundary and absorption condition to truncate the infinite do-

main. Born Approximation is a conventional method in the quantum mechanics and solid physics, however, it is one iteration only in whole domain which is not accurate for high frequency and for high contrast materials. The GL method divides the domain as a set of small sub domains or sub lattices. The Global field is updated by the local field from the interaction between the global field and local subdomain materials successively. Once all subdomain materials are scattered, the GL field solution is obtained which is much more accurate than the Born approximation. GL method is suitable for all frequency and high contrast materials.

Moreover, the GL method can be meshless, including arbitrary geometry subdomains, such as rectangle, cylindrical and spherical coordinate mixed coupled together. It is full parallel algorithm. The GL EM method consistent combines the analytical and numerical approaches together and reduced the numerical dispersion and numerical frequency limitation. The GL method has double capabilities of the theoretical analysis and numerical simulations that has been shown in this paper. Because the cloak metamaterial in (4), (5), and (6) are radial dependent, the reduced one dimension GL EM modeling system by using the sphere harmonic expansion are developed for the cloak simulations. The 3D GL simulations of the EM wave field through the single and multiple sphere, cylinder, ellipsoid, and arbitrary geometry cloaks in single layer and double layer cloaks show that the GLT and GLF EM modeling are accurate, stable and fast. The 3D and 2D GL parallel software are developed and patented by GLGEO.

VII. CONCLUSIONS

Many simulations by the GL modeling and theoretical analysis verify that the EM GL doubled cloak is robust and safe cloak and has complete and sufficient invisibility functions. Its concealment is the normal electromagnetic environment. The outer layer of the GL double layer cloak has the invisible function, its inner layer cloak has fully absorption function. The GL method is an effective physical simulation method. It has double capability of the theoretical analysis and numerical simulations to study the cloak metamaterials and wide material and Field scattering in physical sciences.

Acknowledgments

We wish to acknowledge the support of the GL Geophysical Laboratory. Authors thank to Professor P. D. Lax for his concern and encouragements.

[1] G. Xie, F. Xie, L. Xie, J. Li, PIER 63, 141-152, (2006).

[2] G. Xie, J. Li, L. Xie, F. Xie, Acta Mathematicae Appli-

- cation Sinica, 23, 2, 391-404, (2008).
- [3] G. Xie, J. Li, L. Xie, F. Xie, JEMW, V.20, No. 14, 1991-2000, (2006).
 - [4] J. B. Pendry, D. Schurig, and D. R. Smith, Science, 312,1780 (2006).
 - [5] H. Chen, B. Wu, B. Zhang, A. Kong, PRL, 99, 063903 (2007).
 - [6] C. Argyropoulos, Y.Zhao, Y. Hao, arXiv:0805.2050v1 (2008).
 - [7] S. A. Cummer et al., Phys. Rev. E 74, 036621 (2006).
 - [8] A. Greenleaf, Y. Kurylev, M. Lassas, and G. Uhlmann, Communication Math. Phys. 275, 749 (2007).
 - [9] B. Zhang, H. Chen, BI. Wu, J. Kong, PRL, 100, 063904 (2008).
 - [10] U. Leonhardt and T. Tyc., Broadband invisibility by Non-Euclidean Cloaking, Science 323, 110 (2009)
 - [11] D. Schurig et al, Science 314, 977 (2006)
 - [12] R. Liu et al, Science 323, 366 (2009). bib-item13 J. Li, G. Xie, C.Lin, J. Liu, SEG, Expanded Abstracts, 21, no. 1, 692-695, (2002) <http://www.segdl.org/journals/doc/SEGLIBhome/dci/searchDCI.jsp>
 - [13] G. Xie, J. Li, F. Xie, PIERS2005 in Hangzhou Abstracts, p. 68 (2005) [ISBN: 1-933077-06-9], <http://piers.mit.edu/piersproceedings/piers2k5Proc.php>
 - [14] F. Xie, L. Xie, PIERS2005 in Hangzhou Abstracts, p. 296 (2005) [ISBN: 1-933077-06-9], <http://piers.mit.edu/piersproceedings/piers2k5Proc.php>.